American Journal of Engineering and Applied Sciences

Original Research Paper

Thermal Treatment Effects on the Thermoelectric Properties of Ni/Si/Si + Sb/Si/Si + Ge/Ni Multilayer Thin Films

Satilmis Budak, Zhigang Xiao and Shujun Yang

Department of Electrical Engineering and Computer Science, Alabama A&M University (AAMU), Normal, AL USA

Article history
Received: 02-09-2020
Revised: 12-11-2020
Accepted: 14-11-2020

Corresponding Author:
Satilmis Budak
Department of Electrical Engineering and Computer Science, Alabama A&M University (AAMU), Normal, AL USA
Email: satilmis.budak@aamu.edu

Abstract: The multilayer thermoelectric devices including Ni/200 layers of Si/Si + Sb/200 layers of Si/Si + Ge/Ni thin films were fabricated using electron beam and DC/RF magnetron sputtering deposition systems. The thickness measurements have been performed using Filmetrics UV thickness measurement system. The Au contacts at the bottom and top of the fabricated thermoelectric devices were measured as 100 nm for each side. Ni layer at the bottom is 108 nm and Ni layer at the top of the multilayer structures is 168 nm. The thickness of 200 layers of Si/Si + Ge thin film is 173 nm and the thickness of 200 layers of Si/Si + Sb thin film is 199 nm. The fabricated thermoelectric devices have total of 402 layers of thin films with the total thickness of 648 nm thickness excluding two Au contact layers. The prepared thin film devices were annealed at different temperatures for one hour to improve the thermoelectric properties. The current studied system has reached some remarkable values of Seebeck coefficients when the suitable annealing temperatures and the suitable operating temperatures of Seebeck measurement system were applied. The multilayer thin film system has reached the Seebeck coefficient of -344.8 μV/K when the annealed temperature was 100°C and the operating temperature was 320 K. One of the main problems with the thermoelectric devices is having higher temperature dissipation during the operation of the devices. Ni thin film was used in the fabrication process to remove excess of the heat as a heat sink from the thermoelectric devices. This will bring new approach for the high efficient thermoelectric devices. The goal of the manuscript is to improve the thermoelectric properties of the fabricated thin film thermoelectric devices using Ni thin films and the thermal treatment. The resistivity values decreased when the annealing temperatures increased. The highest power factor values were reached when the thermoelectric devices were annealed at 100°C. Mobility values increased when the suitable temperatures were applied for thermal treatment.

Keywords: Thermoelectric Materials, DC/RF Magnetron Sputtering, Seebeck Coefficient, Thermal Treatment Effects

Introduction

The first important discovery relating to thermoelectricity occurred in 1823 when a German scientist, Thomas Seebeck, found that an electric current would flow continuously in a closed circuit made up of two dissimilar metals provided that the junctions of the metals were maintained at two different temperatures. The Peltier effect was discovered in 1834 by a French watchmaker and part time physicist Jean Charles Athanase Peltier. Peltier found that the use of a current at an interface between two dissimilar materials results in the absorption of heat and release of heat at the subatomic level, this is a result of the different energy levels of materials, particularly *n* and *p* type materials (Jangonda *et al*., 2016).

As we know that most of the heat generated from the various sources is wasted, so in order to minimize the loss, thermoelectricity is a small step towards utilization of this unused/waste heat from various resources. Thermoelectric materials are being used, since few decades, for heat derived electricity generation and for Peltier refrigeration. Thermoelectric materials in general, are small band gap degenerate semiconductors capable in inter-conversion of heat energy and electrical energy (Singh *et al*., 2016).

Science Publications

© 2020 Satilmis Budak, Zhigang Xiao and Shujun Yang. This open access article is distributed under a Creative Commons Attribution (CC-BY) 3.0 license.

DOI: 10.3844/ajeassp.2020.668.682

Solid-state thermoelectric devices are reliable energy converters possessing no noise or vibration, as there are no mechanical moving parts and, therefore, need substantially less maintenance (Chen and Lin, 2019). This provides an edge for thermoelectric to secure an indispensable place in the field of automobile, medical and aerospace applications (MohanKumar *et al.*, 2019). Thermoelectric materials are increasingly becoming more important due to their applications in thermoelectric power generation as heat harvesting and microelectronic cooling devices (Budak *et al.*, 2009a). The efficiency of the thermoelectric devices and materials is determined by the figure of merit, $ZT = S^2\sigma T/\kappa$ where S is the Seebeck coefficient, σ is the electrical conductivity, T is the absolute temperature and κ is the thermal conductivity (Recatala-Gomez *et al.*, 2020; Drabo and Budak, 2019). Improvements in ZT are primarily due to a reduction in lattice thermal conductivity. There are broadly three approaches to reduce lattice thermal conductivity: (a) Phonon scattering, (b) complex crystal structures and (c) nanostructuring. Most of the recent advancements in enhancing ZT is associated with nanostructuring. Because of the quantum size effects on energy carriers, it has been observed that the thermal conductivity of nanostructures such as superlattices is significantly lower than that of the bulk constituent materials (Kishore and Priya, 2018). Thermoelectric parameters are enhanced in structures with reduced dimensionality. As pointed out by Dresselhaus and co-workers in pioneering theoretical works and further investigated also by other authors, the Seebeck coefficient increases in bi-dimensional, or mono-dimensional (nanowires), structures. The Seebeck coefficient strongly depends on the distribution in energy of the charge carriers and in particular it increases when the average difference between the carrier energies and the Fermi energy increases. In low dimensional systems, the density of states is reshaped with respect to bulk systems, in such a way that charge carriers are spread to higher energies (Pennelli, 2014).

The AAMU research approach has been unique in the field of the thermoelectric materials on multi-nano-layered superlattice thin-film systems using MeV ion bombardments to cause nanodots and/or nano-clusters to decrease the thermal conductivity and increase both the Seebeck coefficient and the electrical conductivity. The achieved performance of the devices is remarkable as demonstrated by ZT from the both the cross and in-plane measurements at room temperature (Budak *et al.*, 2009b; 2013). Recent measurements yielded an impressive ZT of 4.9 in SiO_2/SiO_2 + Ge multilayer thin films. Budak *et al.* (2013) performed some researches on Si/Si + Ge (Zheng *et al.*, 2007; Budak *et al.*, 2014) and Si/Si + Sb (Budak *et al.*, 2015a) multilayered thin film modified by high energy ion beam bombardments addition to the researches on different materials. Some suitable fluence (doses) of the applied high energy beam improved the thermoelectric properties of the fabricated multilayer thin film devices. Budak *et al.* (2015b) also performed some researches on the thermal treatment effects on the thermoelectric properties of thermoelectric devices (Budak *et al.*, 2017; 2015b). Like the ion beam bombardment, thermal annealing caused similar improvements on the thermoelectric properties of the fabricated thermoelectric devices since thermal annealing caused nano-cluster structures forming (Güner *et al.*, 2014) in the layers to increase the Seebeck coefficients and the electrical conductivity and decrease in the thermal conductivity values at suitable annealing temperatures. Due to the motivation of success in high energy ion beam and temperature annealing on the material systems, this study aims to perform thermal annealing effects on the multilayer thin films to see how their thermoelectric properties are effected from the thermal treatment at different temperatures. One of the main problems with the thermoelectric devices is having higher temperature dissipation during the operation of the devices. Ni thin film was selected and used in the fabrication process to remove excess of the heat as a heat sink from the thermoelectric devices. This will bring new approach for the high efficient thermoelectric devices. The goal of the manuscript is to improve the thermoelectric properties of the fabricated thin film thermoelectric devices using Ni thin films and thermal treatment.

Experimental

The thermoelectric devices including Ni/200 layers of Si/Si + Sb/200 layers of Si/Si + Ge/Ni thin films were fabricated using electron beam and DC/RF magnetron sputtering deposition systems. The used geometry is shown in Fig. 1. The fabricated multilayer thin film devices were sandwiched by Au contacs both at the bottom and top of the fabricated structures for the measurements. The thickness measurements have been performed using Filmetrics UV thickness measurement system. The Au contacts at the bottom and top of the fabricated was measured as 100 nm for each side. Ni layer at the bottom is 108 nm and Ni layer at the top of the multilayer structures is 168 nm. As seen from Fig. 1, the thickness of 200 layers of Si/Si + Ge thin film is 173 nm and the thickness of 200 layers of Si/Si + Sb thin film is 199 nm. The total thickness of the fabricated device shown in Fig. 1 is 848 nm including two layers of Au at the bottom and the top. The thin film samples used for the van der Pauw measurements and the Seebeck coefficients do not have Au contacts at the bottom and the top of the multilayered thin films.

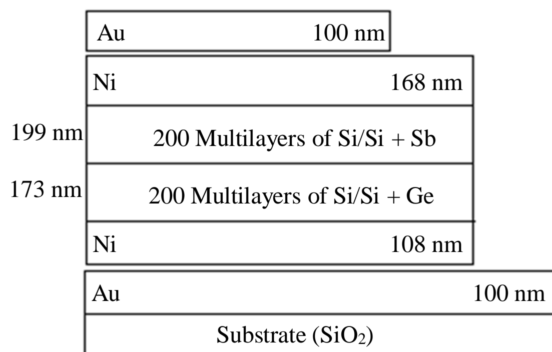

Fig. 1: Used geometry for multilayer thermoelectric devices

The fabricated thin film devices annealed at different temperatures from 100 to 600°C have been characterized using the Seebeck coefficient measurement system, the van der Pauw 4-probe measurement system and SEM/EDS measurement system. Van der Pauw measurement system was used for electrical resistivity, mobility, density, Hall Effect and sheet resistance measurements. Conductivity values were calculated via taking the reciprocal of the resistivity values.

Results and Discussion

Figure 2 shows the temperature dependence of the Seebeck coefficients for Ni/200 layers of Si/Si + Sb/200 layers of Si/Si + Ge/Ni thin films. As seen from Fig. 2, the Seebeck coefficients including unannealed and annealed ones from 100 to 400°C have been measured when the operating temperature changed from 300 to 380 K. Seebeck values increased in negative direction since the material system behaves like a n-type semiconductor material when the suitable annealing and operating temperatures were applied. A good thermoelectric material should have a Seebeck coefficient value changing between 100 and 300 μV/K; thus, in order to achieve a few volts at the load, many thermoelectric couples need to be connected in series to make the efficient thermoelectric devices (Purhoit *et al.*, 2016). The current studied system has reached some remarkable values of the Seebeck coefficients when the suitable annealing and operating temperatures were introduced. The multilayer thin film system has reached the Seebeck coefficient of -344.8 μV/K for the when the annealed temperature was 100°C and the operating temperature of the Seebeck measurement system was 320 K. This is a very high remarkable Seebeck coefficient value according to the literature (Purhoit *et al*., 2016). The multilayer system has reached also some other higher Seebeck coefficient values of -290.07 μV/K when the annealed temperature was 100°C and the operating temperature was 360 K; -229.04 μV/K when the annealed temperature was 400°C and the operating temperature was 360 K; -295.16 μV/K when the annealed temperature was 400°C and the operating temperature was 380 K. As seen from Fig. 2, there are many other good Seebeck coefficient values over -100 μV/K. These multilayer thin film systems have shown remarkable high Seebeck coefficient values due to the selection of different material systems and using Ni thin films for removing of an excess of heat during the operation of the thermoelectric device. The high Seebeck coefficient might come from due to the interfacal reaction between Ni and other deposited multilayer thin films (Guo *et al*., 2019).

Figure 3 shows the thermal treatment dependence of the Seebeck coefficients for Ni/200 layers of Si/Si + Sb/200 layers of Si/Si + Ge/Ni thin films. As seen from Fig. 3, the efficient annealing temperatures for higher Seebeck coefficients could be seen easily at the axis of annealing temperature since the Seebeck coefficient peak values could be seen concentrated at those efficient annealing temperatures. Figure 3 brings a clarification of measured Seebeck coefficient values while x-axis is showing annealed temperatures and y-axis is showing Seebeck coefficient values. For each of the annealed temperatures, there are five different values of Seebeck coefficients for different operating temperatures.

Figure 4 shows the thermal treatment dependence of the square of the Seebeck coefficients for Ni/200 layers of Si/Si + Sb/200 layers of Si/Si + Ge/Ni thin films. In Fig. 4, the values of squares of the Seebeck coefficients were plotted with respect to the annealing temperatures to show the behavior of the Seebeck coefficient in the Figure of merit calculations and the power factor calculation. Figure 5 shows the temperature dependence of the resistivity for Ni/200 layers of Si/Si + Sb/200 layers of Si/Si + Ge/Ni thin films. Resistivity measurements have been performed using the van der Pauw four probe measurement system at the operation temperature changing from 300 K (about 27°C) to 500 K (about 227°C). As seen from Fig. 5, there are four different thermoelectric devices including annealed and unannealed devices. The resistivity values for each thermoelectric device slightly change when the operation temperature changed from 300 K (about 27°C) to 500 K (about 227°C). But, not too much deviations or changes have been seen. As seen from the resistivity curves for each different thermoelectric device, the resistivity values decreased when the annealing temperatures increased. This is a very remarkable result since the good thermoelectric material have lower electrical resistivity or higher electrical conductivity (Güner *et al*., 2014).

Figure 6 shows the thermal treatment dependence of the resistivity for Ni/200 layers of Si/Si + Sb/200 layers of Si/Si + Ge/Ni thin films for unannealed and annealed samples up to 300°C. The explanations from Fig. 5 were shown more clearly at Fig. 6. As seen from Fig. 6, the resistivity values decreased when the annealing temperature increased. Each individual curve belongs to the different operation temperature changing from 300 K (about 27°C) to 500 K (about 227°C).

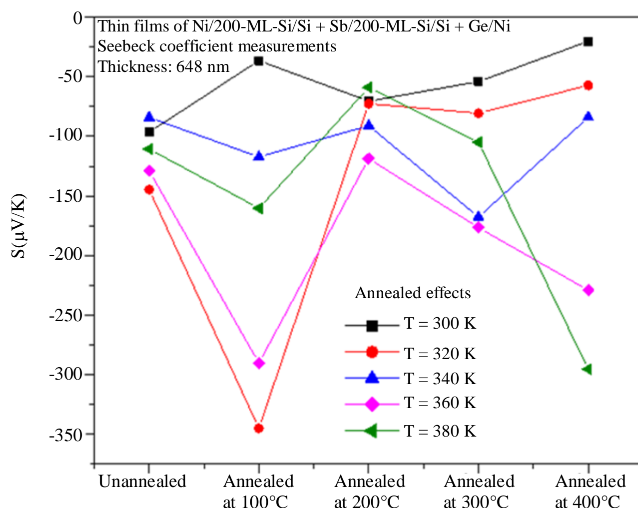

Fig. 2: Temperature dependence of the Seebeck coefficients for Ni/200 layers of Si/Si + Sb/200 layers of Si/Si + Ge/Ni thin films

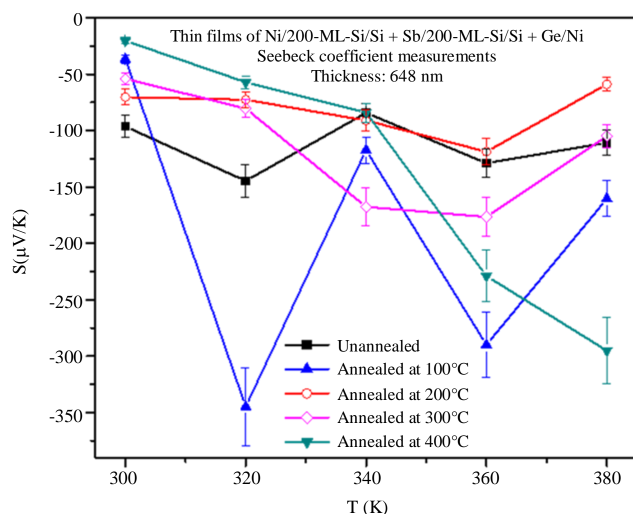

Fig. 3: Thermal treatment dependence of the Seebeck coefficients for Ni/200 layers of Si/Si + Sb/200 layers of Si/Si + Ge/Ni thin films

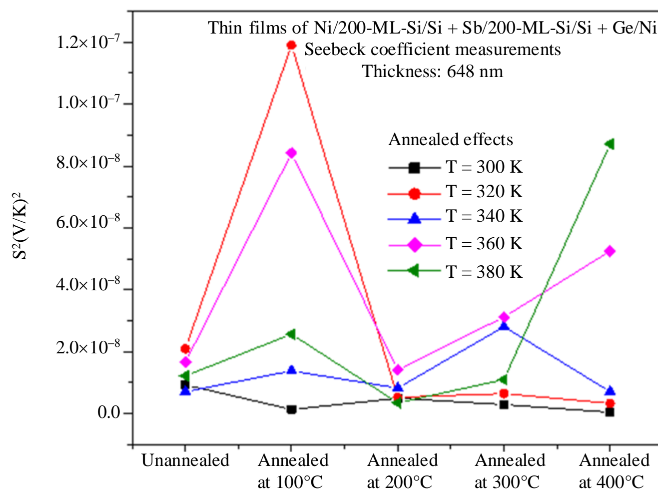

Fig. 4: Thermal treatment dependence of the square of the Seebeck coefficients for Ni/200 layers of Si/Si + Sb/200 layers of Si/Si + Ge/Ni thin films

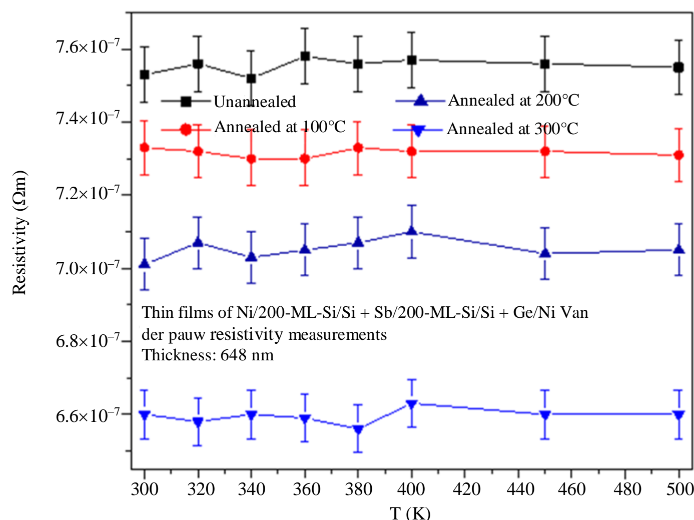

Fig. 5: Temperature dependence of the resistivity for Ni/200 layers of Si/Si + Sb/200 multilayers of Si/Si + Ge/Ni thin films

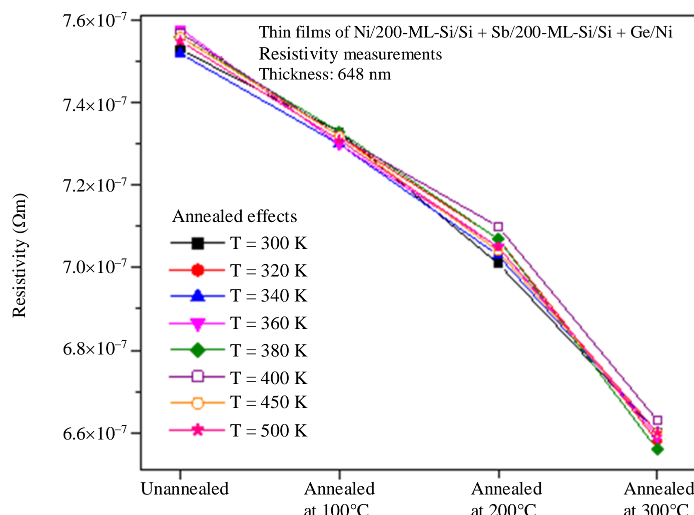

Fig. 6: The thermal treatment dependence of the resistivity for Ni/200 layers of Si/Si + Sb/200 layers of Si/Si + Ge/Ni thin films for unannealed and annealed samples up to 300°C

Figure 7 is an expanded temperature version of Fig. 6 for the thermoelectric devices from unannealed case to annealed 600°C cases. Due to the sharp and high amount of increase in resistivity at the thermoelectric devices annealed at 500°C, the resistivity values look overlapped to each other. Figure 8 shows the temperature dependence of the electrical conductivity values for Ni/200 layers of Si/Si + Sb/200 layers of Si/Si + Ge/Ni thin films. Electrical conductivity results have been computed by taking the reciprocal of the resistivity values given in Fig. 5. As seen from Fig. 8, there are four different thermoelectric devices including annealed and unannealed ones. The electrical conductivity values for each thermoelectric device slightly change during the operation temperature from 300 K (about 27°C) to 500 K (about 227°C). But, too much deviations or changes have not been seen. As seen from the conductivity curves for each different thermoelectric device, the electrical conductivity values increased when the annealing temperatures increased. This is a very remarkable result since the good thermoelectric materials have higher electrical conductivity values (Güner *et al.*, 2014).

Figure 9 shows the thermal treatment dependence of the electrical conductivity for Ni/200 layers of Si/Si + Sb/200 layers of Si/Si + Ge/Ni thin films for unannealed and annealed devices with the annealing temperatures changing up to 300°C. The explanation introduced at Fig. 8 was seen more clearly at Fig. 9 while the electrical conductivity values were plotted with respect the annealing temperatures. As seen from Fig. 9, the electrical conductivity values increased when the annealing temperature increased. Each individual curve shows the

behavior of the electrical conductivity dependence at the different operation temperature changing from 300 K (about 27°C) to 500 K (about 227°C).

Figure 10 shows the thermal treatment dependence of the electrical conductivity for Ni/200 layers of Si/Si + Sb/200 layers of Si/Si + Ge/Ni thin films. Figure 10 is an extended temperature version of Fig. 9. Since there is a sharp and high amount of decrease in the electrical conductivity at the thermoelectric devices annealed at 400°C, the electrical conductivity values look overlapped to each other.

Figure 11 shows the thermal treatment dependence of the power factor for Ni/200 layers of Si/Si + Sb/200 layers of Si/Si + Ge/Ni thin films. Power factor can be found with the multiplication of the square of the Seebeck coefficient with the conductivity values. Power factor is used to give an idea about the efficiency of the thermoelectric devices. As mentioned at the introduction part of this manuscript, the Figure of merit, *ZT*, depends on the power factor. In addition, the thermal conductivity value divides the power factor and the results of the division should be multiplied by the absolute temperatures. In some cases, the measurements of the thermal conductivity of the thin films are very difficult. That is why, power factor is a symbol of the efficiency for the thermoelectric materials and devices. As seen from Fig. 11, the highest power factor values reached when the thermoelectric devices were annealed at 100°C.

Figure 12 shows the temperature dependence of the mobility for Ni/200 layers of Si/Si + Sb/200 layers of Si/Si + Ge/Ni thin films. As seen from Fig. 12, the mobility values increased when the suitable temperatures were applied for the thermal treatment. The highest values of the mobility were reached between 320 and 360 K when the multilayer thin films were annealed at 100 and 500°C. In addition, the increase in mobility could be seen at different annealed temperatures from 300 K (about 27°C) to 500 K (about 227°C). This shows that the suitable thermal treatment could cause higher mobility for the thermoelectric materials. Figure 13 shows the log-linear graph of the temperature dependence of the mobility for Ni/200 layers of Si/Si + Sb/200 layers of Si/Si + Ge/Ni thin films. Addition to the Fig. 12, more details could be seen clearly in Fig. 13 by using log-linear plotting. The over-lapping data due to the scale usage in Fig. 12 were plotted and expanded in detail to give readers more clear explanation of experimental data. Figure 14 shows the thermal treatment dependence of the mobility for Ni/200 layers of Si/Si + Sb/200 layers of Si/Si + Ge/Ni thin films. The difference of the Fig. 14 with respect the Fig. 12 and 13 is the x-axis showing the annealed temperatures. The thermal treatment values were plotted like independent parameter for the mobility values with respect to the operation temperatures changing from 300 K (about 27°C) to 500 K (about 227°C). As seen from Fig. 14, the highest peaks reached when the thin film materials were annealed at 100 and 500°C.

Figure 15 shows the temperature dependence of the density for Ni/200 layers of Si/Si + Sb/200 layers of Si/Si + Ge/Ni thin films. Figure 16 shows the thermal treatment dependence of the density for Ni/200 layers of Si/Si + Sb/200 layers of Si/Si + Ge/Ni thin films. As seen from Fig. 16, the density values dropped when the multilayer thin films were annealed at 400°C. The density values from unannealing to annealing at 600°C could be seen clearly.

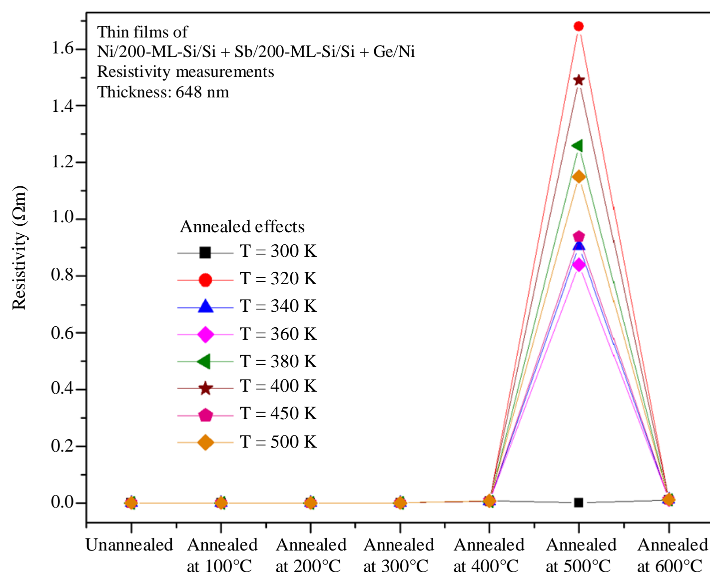

Fig. 7: Thermal treatment dependence of the resistivity for Ni/200 layers of Si/Si + Sb/200 layers of Si/Si + Ge/Ni thin films

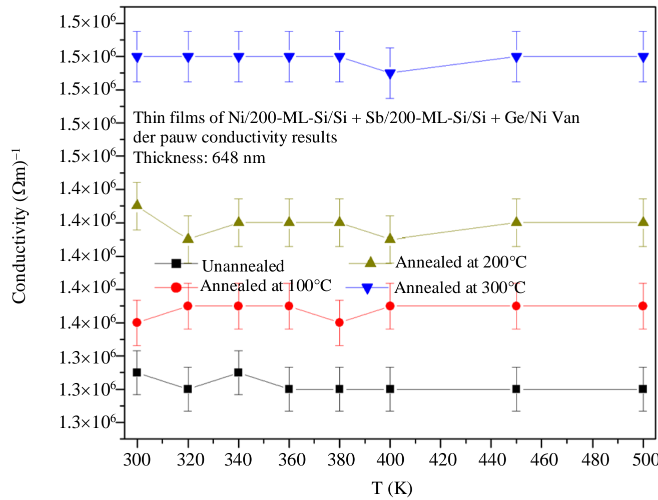

Fig. 8: Temperature dependence of the electrical conductivity for Ni/200 layers of Si/Si + Sb/200 multilayers of Si/Si + Ge/Ni thin films

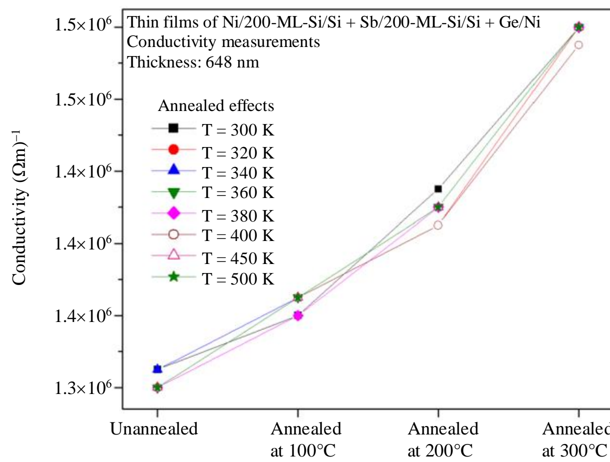

Fig. 9: Thermal treatment dependence of the conductivity for Ni/200 layers of Si/Si + Sb/200 layers of Si/Si + Ge/Ni thin films for unannealed and annealed samples up to 300°C

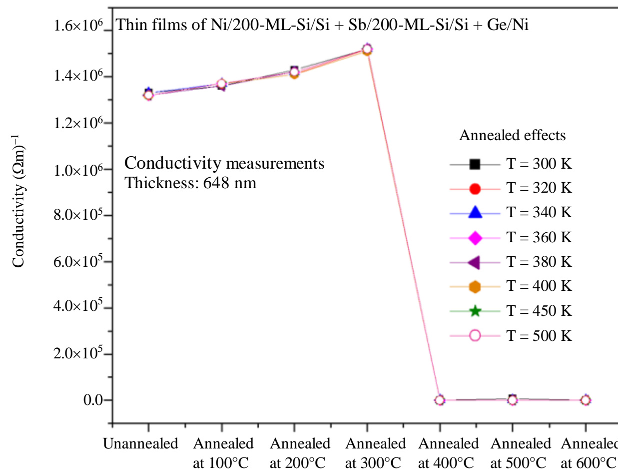

Fig. 10: Thermal treatment dependence of the conductivity for Ni/200 layers of Si/Si + Sb/200 layers of Si/Si + Ge/Ni thin films

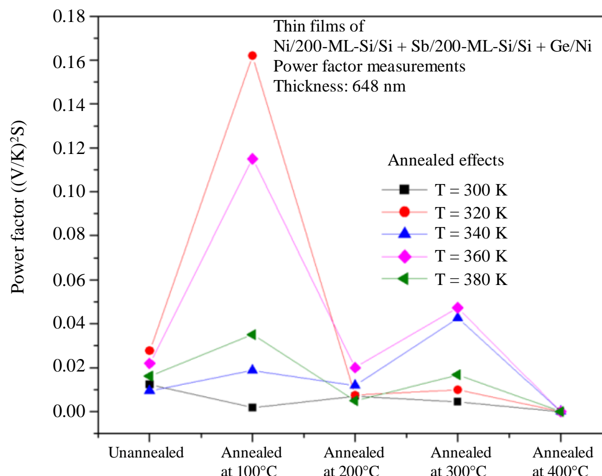

Fig. 11: Thermal treatment dependence of the power factor for Ni/200 layers of Si/Si + Sb/200 layers of Si/Si + Ge/Ni thin films

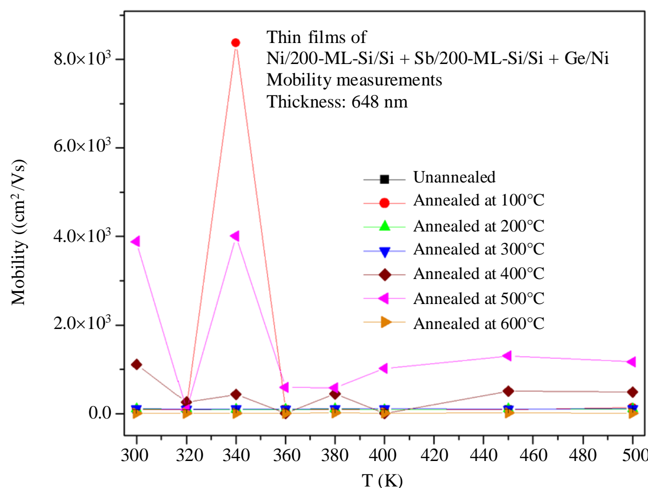

Fig. 12: Temperature dependence of the mobility for Ni/200 layers of Si/Si + Sb/200/ layers of Si/Si + Ge/Ni thin films

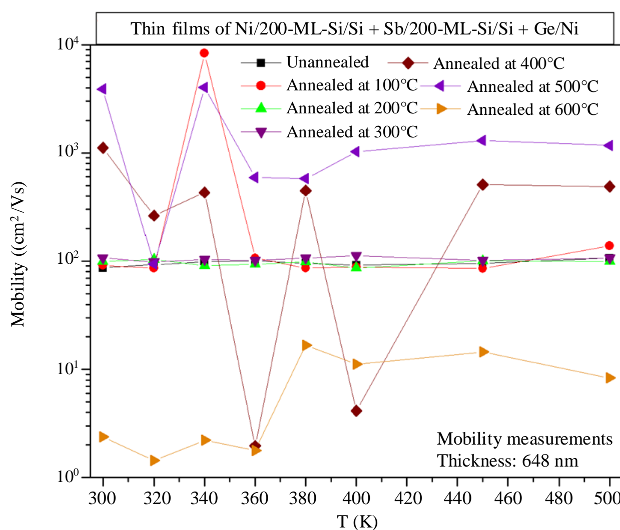

Fig. 13: Log-linear graph of the temperature dependence of the mobility for Ni/200 layers of Si/Si + Sb/200 layers of Si/Si + Ge/Ni thin films

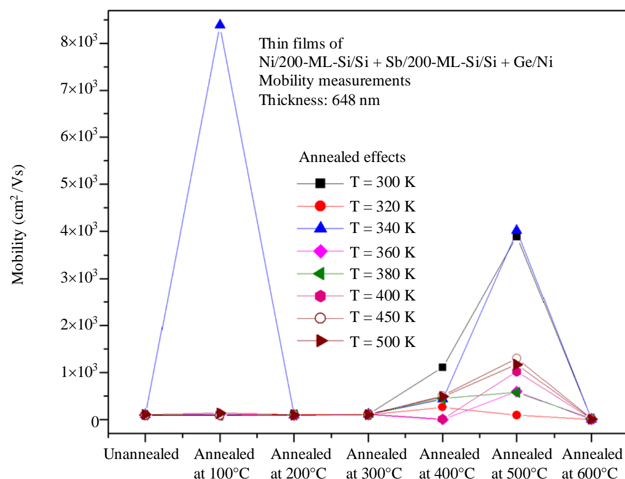

Fig. 14: Thermal treatment dependence of the mobility for Ni/200 layers of Si/Si + Sb/200 layers of Si/Si + Ge/Ni thin films

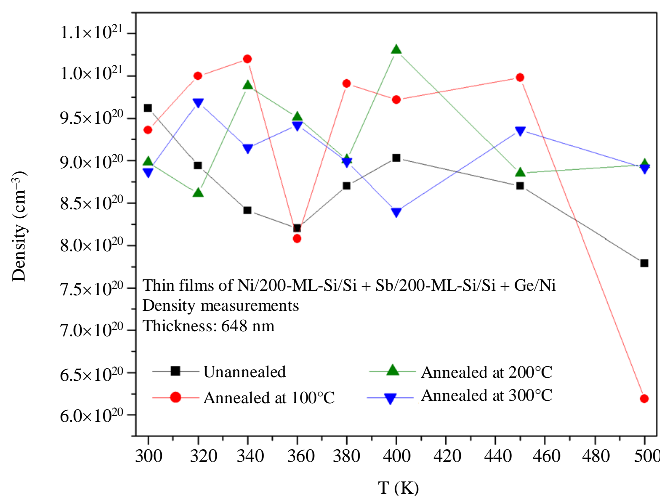

Fig. 15: Temperature dependence of the density for Ni/200 layers of Si/Si + Sb/200 layers of Si/Si + Ge/Ni thin films

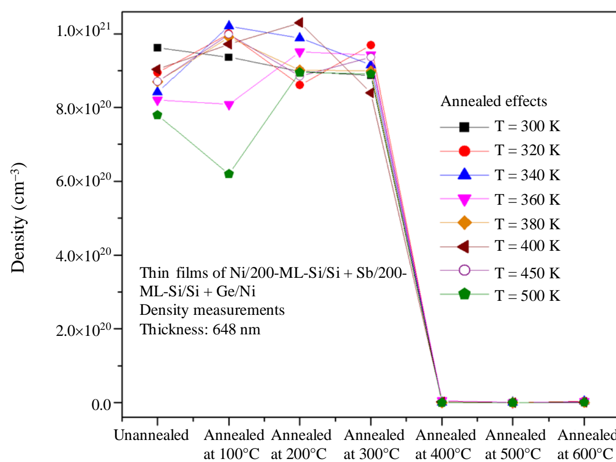

Fig. 16: Thermal treatment dependence of the density for Ni/200 layers of Si/Si + Sb/200 layers of Si/Si + Ge/Ni thin films

Figure 17 shows the temperature dependence of the Hall Effect coefficients for Ni/200 layers of Si/Si + Sb/200 layers of Si/Si + Ge/Ni thin films from the unannealed case up to the annealed at 300°C case. Except for 100°C, the Hall Effect values changed between 6×10^{-3} to 8×10^{-3} cm^3/C. The thin film annealed at 100°C has reached the highest Hall Effect coefficient when the operation temperature was 500 K. This could come from the materials effectiveness at higher operation temperatures under the applied magnetic field. As the other cases including unannealed case have reached higher values of the Hall Effect coefficient at 500 K, the annealing at 100°C caused higher values with respect to the others. For the future studies, thermal treatment could be performed between unannealed case to 100°C in with more detailed of temperature increment to clarify the annealing effects on the Hall Effect coefficient for this material system.

Figure 18 shows the log-linear graph of the temperature dependence of the Hall Effect coefficients for Ni/200 layers of Si/Si + Sb/200 layers of Si/Si + Ge/Ni thin films for the unannealed case up to annealed at 600°C case. Since the log-linear graph plotting was used to show all the annealed temperatures, Fig. 18 shows more data than Fig. 17. As seen from Fig. 18, except for 500°C, the other cases caused lower Hall Effect coefficients.

Figure 19 shows the thermal treatment dependence of the Hall Effect coefficients for Ni/200 layers of Si/Si + Sb/200 layers of Si/Si + Ge/Ni thin films. As seen from Fig. 19, all annealed temperatures have been shown on the graph while the operation temperature has changed from 300 K (about 27°C) to 500 K (about 227°C). The thin film annealed at 500°C have higher values with respect to the other cases.

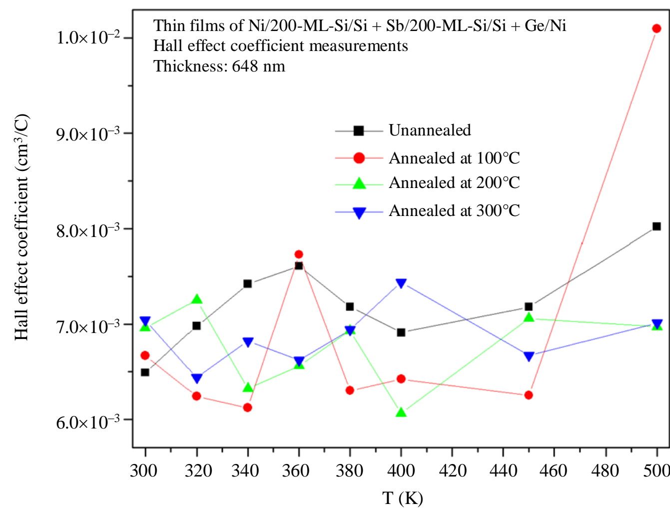

Fig. 17: Temperature dependence of the Hall Effect coefficients for Ni/200 layers of Si/Si + Sb/200 layers of Si/Si + Ge/Ni thin films

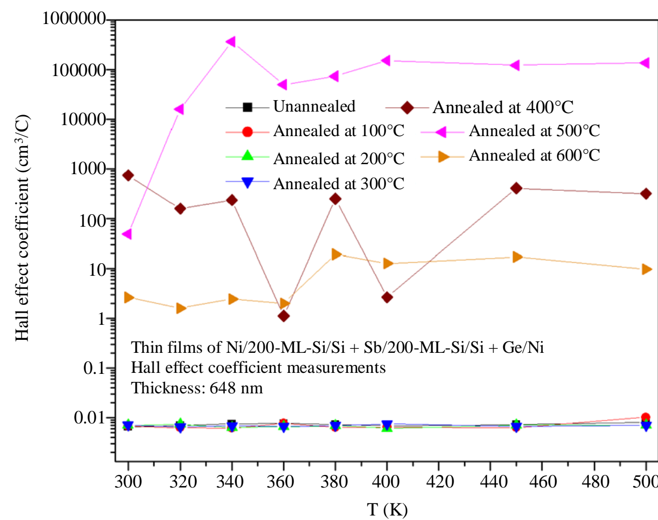

Fig. 18: Log-linear graph of the temperature dependence of the hall effect coefficients for Ni/200 layers of Si/Si + Sb/200 layers of Si/Si + Ge/Ni thin films

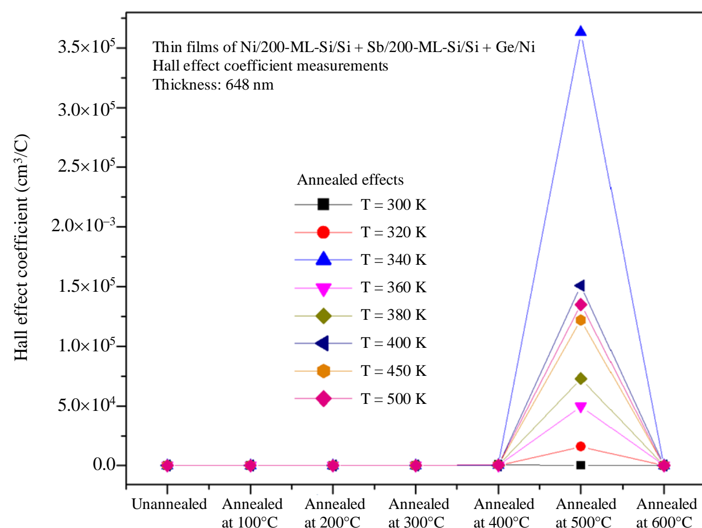

Fig. 19: Thermal treatment dependence of the Hall Effect coefficients for Ni/200 layers of Si/Si + Sb/200 layers of Si/Si + Ge/Ni thin films

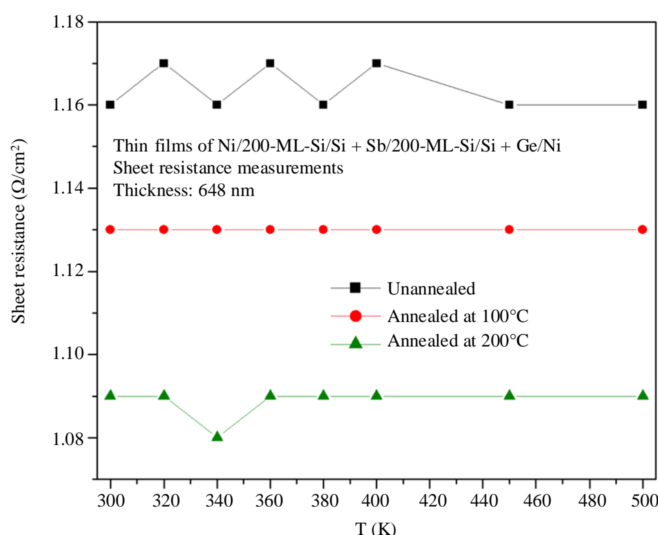

Fig. 20: Temperature dependence of the sheet resistance for Ni/200 layers of Si/Si + Sb/200 layers of Si/Si + Ge/Ni thin films for unannealed, annealed at 100°C and 200°C cases

Figure 20 shows the temperature dependence of the sheet resistance for Ni/200 layers of Si/Si + Sb/200 layers of Si/Si + Ge/Ni thin films for unannealed, annealed at 100 and 200°C cases. Figure 21 shows the temperature dependence of the sheet resistance for Ni/200 layers of Si/Si + Sb/200 layers of Si/Si + Ge/Ni thin films for annealed at 300, 400 and 600°C cases. Sheet resistance values decreased when the thin films were annealed up to 200°C as seen in Fig. 20. This is a very good behavior for the good thermoelectric materials and devices. When the thin films were annealed at 300, 400 and 600°C, the sheet resistance values increased as seen in Fig. 21. Both Fig. 20 and 21 show about the stability for sheet resistance while the operation temperature of the van der Pauw four probe measurement system were being increased from 300 to 500 K. This stability shows the sheet resistance values did not fluctuate very much when the environmental temperature changes. This might give idea for this material that it could be used in the temperature interval from 300 K (about 27°C) to 500 K (about 227°C).

Figure 22 shows the thermal treatment dependence of the sheet resistance for Ni/200 layers of Si/Si + Sb/200 layers of Si/Si + Ge/Ni thin films. All cases from unannealed to annealed for 100°C to 600°C were plotted on the graph with the operation temperatures changing from 300 K to 500 K. As seen from Fig. 22, the highest sheet resistance value for all operation temperatures were reached when the thin film was annealed at 500°C.

As discussed in Fig. 20, the sheet resistance values decreased when the thin films were annealed up to 200°C. To show the annealing effects on the sheet resistance, the sheet resistance values were plotted with respect to the annealing temperatures while the operation temperature changed from 300 K (about 27°C) to 500 K (about 227°C). Figure 23 shows the effect of the thermal treatments on the sheet resistance. When the thermal treatment was introduced, the sheet resistance values decreased for all operation temperatures. This is a very good sign for the high efficient thermoelectric devices since the expectation for the good thermoelectric devices and materials is having high Seebeck coefficient and lower electrical resistivity and low thermal conductivity.

Figure 24 shows the SEM micrographs for Ni/200 layers of Si/Si + Sb/200 layers of Si/Si + Ge/Ni thin films for unannealed, annealed at 200, 400 and 600°C cases. The surface micrographes except for the case annealed at 600°C, look quite smooth. When the annealing temperature reached 600°C, the surface morphology started to change. This might come due to the changes in the weight percentage for O and Ni as seen from Table 1.

Table 1 shows the EDS analysis for the percentages of weights for Ni/200 layers of Si/Si + Sb/200 layers of Si/Si + Ge/Ni thin films for annealed at 200, 300, 400, 500 and 600°C cases. As seen from Table 1, the percentage of weight of O increased while the percentage of weight of Ni decreased when the thin films were being annealed from 200 to 600°C. The EDS results for unannealed case could not be gathered. That is why the results from unannealed cases have not been shown in Table 1. But the changes in the percentage of weight for O and Ni for the different annealing temperatures showed clear understanding on how O and Ni levels were depending on the temperature treatment.

Table 1: EDS analysis for percentages of weights of Ni/200 layers of Si/Si + Sb/200 layers of Si/Si + Ge/Ni thin films for annealed at 200, 300, 400, 500 and 600°C cases Annealed

Temperature (°C)	Weight % for O	Weight % for Ni
200	06.43	93.57
300	06.49	94.31
400	06.98	93.02
500	08.13	91.87
600	23.49	76.51

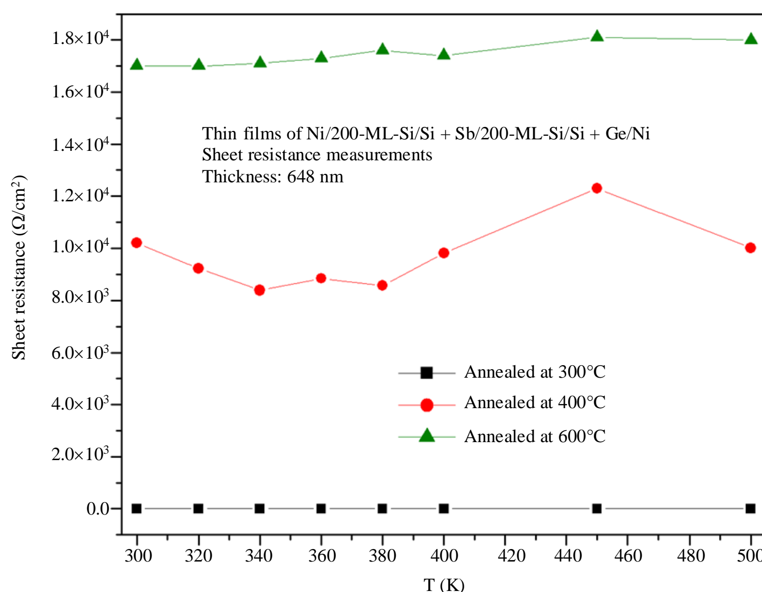

Fig. 21: Temperature dependence of the sheet resistance for Ni/200 layers of Si/Si + Sb/200 layers of Si/Si + Ge/Ni thin films for annealed at 300, 400 and 600°C cases

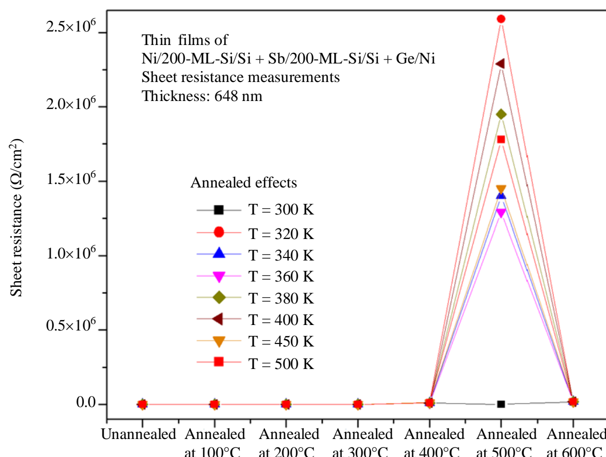

Fig. 22: Thermal treatment dependence of the sheet resistance for Ni/200 layers of Si/Si + Sb/200 layers of Si/Si + Ge/Ni thin films

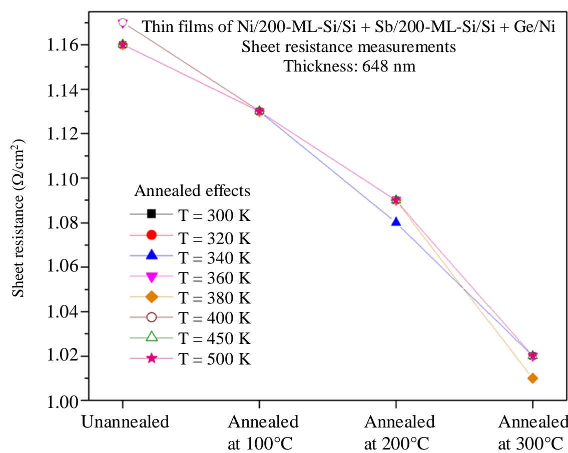

Fig. 23: Thermal treatment dependence of the sheet resistance for Ni/200 layers of Si/Si + Sb/200 layers of Si/Si + Ge/Ni thin films for unannealed and annealed samples up to 300°C

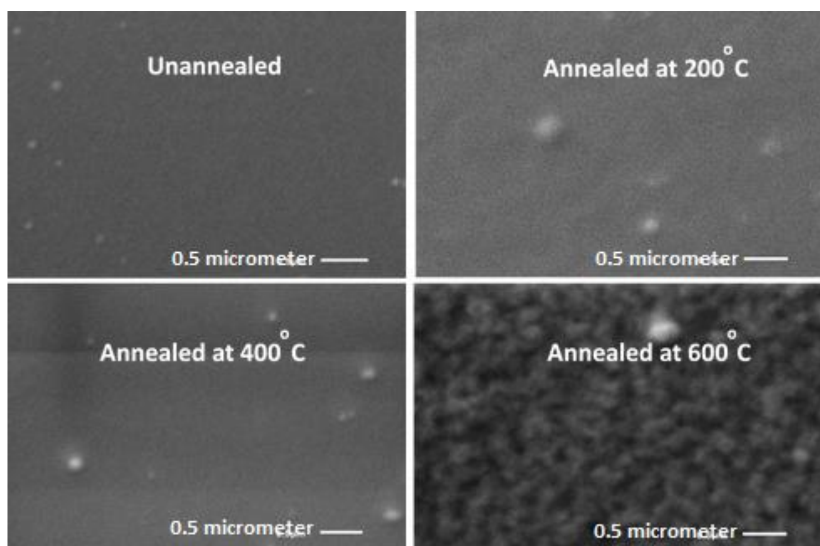

Fig. 24: SEM micrographs for Ni/200 layers of Si/Si + Sb/200 layers of Si/Si + Ge/Ni thin films for unannealed, annealed at 200°C, 400°C and 600°C cases

Future Perspective

One of the problems for the high efficient thermoelectric devices is having an excess of heat during the operation. The current material systems reached remarkable Seebeck coefficient at the suitable annealing temperatures and the operation temperatures. Ni layers used for both at the top and bottom of the fabricated devicess could cause removing of heat from the thermoelectric devices during operation and the high Seebeck coefficient might come from due to the interfacial reaction between Ni and other deposited multilayer thin films (Guo *et al*., 2019). For the future works, the thickness of Ni and annealing temperatures could be changed and results could be compared to each other. Addition to the experimental analysis, some theoretical modeling analysis and statistical analysis could be performed by the collaboration with colleagues from different disciplines to understand the behavior of the thermoelectric systems in different perspectives. Addition to the Seebeck coefficient and the electrical conductivity measurements for the calculation of the figure of merit, *ZT*, the thermal conductivity measurements could be performed.

Conclusion

The thermoelectric devices including Ni/200 layers of Si/Si + Sb/200 layers of Si/Si + Ge/Ni thin films were fabricated using electron beam and DC/RF magnetron sputtering deposition systems. The thickness measurements have been performed using the Filmetrics UV thickness measurement system. The Au contacts at the bottom and at the top of the fabricated thin film systems were measured as 100 nm for each side. Ni layer at the bottom is 108 nm and Ni layer at the top of the multilayer structures is 168 nm. The thickness of 200 layers of Si/Si+Ge thin film is 173 nm and the thickness of 200 layers of Si/Si + Sb thin film is 199 nm. The fabricated thermoelectric devices have total of 402 layers of deposition of thin films with the total thickness of 648 nm excluding two Au contact layers. The current studied system has reached some remarkable values of the Seebeck coefficients when the suitable annealing temperatures and suitable operating temperatures were applied. The multilayer thin film system has reached the Seebeck coefficient value of -344.8 μV/K when the annealed temperature was 100°C and the operating temperature was 320 K. Resistivity measurements have been performed using van der Pauw four probe measurement system at the operation temperature changing from 300 K (about 27°C) to 500 K (about 227°C) to see the temperature dependence of the fabricated thermoelectric devices. The resistivity values decreased when the annealing temperatures increased. The highest power factor values were reached when the thermoelectric devices were annealed at 100°C. Mobility values increased when the suitable temperatures were applied for thermal treatment. The highest values of the mobility were reached between 320 K and 360 K when the multilayer thin films were annealed at 100 and 500°C. Except for the annealing temperature of 100°C, the Hall Effect values changed between 6×10^{-3} to 8×10^{-3} cm^3/C. The thin film annealed at 100°C has reached the highest Hall Effect coefficient when the operation temperature was 500 K. When the thermal treatment was introduced, the sheet resistance values decreased for all operation temperatures. The surface micrographes except for the case annealed at 600°C, look quite smooth. When the annealing temperature reached 600°C, the surface morphology started to change. This might come due to the changes in the percentages of weights for O and Ni.

Acknowledgement

The author would like to thank Dr. M. Alim for his contribution to the Department of Electrical Engineering and Computer Science for bringing SEM/EDX system as a PI on his grant.

Funding Information

This project was supported by DOE/NNSA with Contract# DE-NA0001896 and DE-NA0002687; NSF-HBCU-RISE with the proposal number of 1546965.

Author's Contributions

All authors equally contributed in this study.

Ethics

All rights reserved. No part of this publication may be reproduced or transmitted in any form or by any means, electronic or mechanical, including photocopy, or any information storage and retrieval system, without permission in writing from the publisher or authors.

References

Budak, S., Gulduren, E., Allen, B., Cole, J., Lassiter, J., Colon, T., ... & Johnson, R. B. (2015a). High Energy Radiation Effects on the Seebeck Coefficient, van der Pauw-Hall Effect Parameters and Optical Properties of Si/Si+ Sb Multi-Nanolayered Thin Films. American Journal of Materials Science, 5(3A), 39-47.

Budak, S., Baker, M., Lassiter, J., Smith, C., Muntele, C., & Johnson, R. B. (2015b). Effects of Thermal Annealing on the Thermoelectric and Optical Properties of SiO 2/SiO 2+ Cu Nanolayer Thin Films. Journal of Electronic Materials, 44(6), 1420-1425.

Budak, S., Guner, S., Muntele, C., & Ila, D. (2009a). MeV Si ion beam modification effects on the thermoelectric generator from Er0. 1Fe1. 9SbGe0. 4 thin film. Nuclear Instruments and Methods in Physics Research Section B: Beam Interactions with Materials and Atoms, 267(8-9), 1592-1595.

Budak, S., Guner, S., Smith, C., Minamisawa, R. A., Zheng, B., Muntele, C., & Ila, D. (2009b). Surface modification of Si/Ge multi-layers by MeV Si ion bombardment. Surface and Coatings Technology, 203(17-18), 2418-2421.

Budak, S., Heidary, K., Johnson, R. B., Colon, T., Muntele, C., & Ila, D. (2014). MeV Si ion modifications on the thermoelectric generators from Si/Si+ Ge superlattice nano-layered films. Applied surface science, 310, 221-225.

Budak, S., Parker, R., Smith, C., Muntele, C., Heidary, K., Johnson, R. B., & Ila, D. (2013). Superlattice multinanolayered thin films of SiO_2/SiO_2+ Ge for thermoelectric device applications. Journal of intelligent material systems and structures, 24(11), 1357-1364.

Budak, S., Xiao, Z., Cole, J., Price, D., Davis, T., Strong, T., & Alim, M. A. (2017). Thermoelectric and optical properties of advanced thermoelectric devices from $Ni/Bi_2Te_3/Ni$ and $Ni/Sb_2Te_3/Ni$ thin films. Journal of Vacuum Science & Technology B, Nanotechnology and Microelectronics: Materials, Processing, Measurement and Phenomena, 35(5), 051401.

Chen, W. H., & Lin, Y. X. (2019). Performance comparison of thermoelectric generators using different materials. Energy Procedia, 158, 1388-1393.

Drabo, M., & Budak, S. (2019) "Thermoelectric and Optical Properties of Advanced Thermoelectric Devices from Different Multilayer Thin Films", American Journal of Applied Sciences, 16 (8): 225.237.

Güner, S., Budak, S., Gibson, B., & Ila, D. (2014). Optical properties of Ag nanoclusters formed by irradiation and annealing of SiO2/SiO2: Ag thin films. Applied surface science, 310, 180-183.

Guo, X., Zhu, W., Xing, L., Mu, X., Li, C., Ma, S., ... & Zhao, W. (2019). Preparation and Characterization of Ni/Bi 0.5 Sb 1.5 Te 3 Heterogeneous Multilayered Thermoelectric Materials. Journal of Electronic Materials, 1-9.

Jangonda, C., Patil, K., Kinikar, A., Bhokare, R., & Gavali, M. D. (2016). Review of Various Application of Thermoelectric Module. Intl. J. Innovative Research in Science, Engineering and Technology, 5(3), 3393.

Kishore, R. A., & Priya, S. (2018). A review on low-grade thermal energy harvesting: Materials, methods and devices. Materials, 11(8), 1433.

MohanKumar, P., Jagadeesh Babu, V., Subramanian, A., Bandla, A., Thakor, N., Ramakrishna, S., & Wei, H. (2019). Thermoelectric materials-strategies for improving device performance and its medical applications. Sci, 1(2), 37.

Pennelli, G. (2014). Review of nanostructured devices for thermoelectric applications. Beilstein Journal of Nanotechnology, 5(1), 1268-1284.

Purhoit, K., Meena, P. M., & Singh, K. (2016). Review paper on optimizations of thermoelectric system. International J Innov Res Eng Manag, 3, 259-263.

Recatala-Gomez, J., Suwardi, A., Nandhakumar, I., Abutaha, A., & Hippalgaonkar, K. (2020). Toward Accelerated Thermoelectric Materials and Process Discovery. ACS Applied Energy Materials, 3(3), 2240-2257.

Singh, N. K., Bathula, S., Gahtori, B., Tyagi, K., Haranath, D., & Dhar, A. (2016). The effect of doping on thermoelectric performance of p-type SnSe: Promising thermoelectric material. Journal of Alloys and Compounds, 668, 152-158.

Zheng, B., Budak, S., Zimmerman, R. L., Muntele, C., Chhay, B., & Ila, D. (2007). Effect of layer thickness on thermoelectric properties of multilayered Si1- xGex/Si after bombardment by 5 MeV Si Ions. Surface and Coatings Technology, 201(19-20), 8531-8533.